Numerical Simulation and X-ray Imaging Validation of Wormhole Propagation during Acid Core-Flood Experiments in a Carbonate Gas Reservoir

Accepted Manuscript

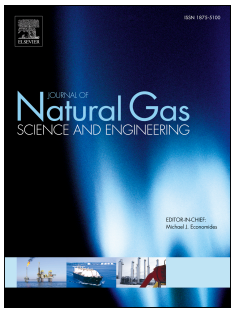

Numerical Simulation and X-ray Imaging Validation of Wormhole Propagation during Acid Core-Flood Experiments in a Carbonate Gas Reservoir

Alireza Safari, Mojtaba Moradi Dowlatabad, Ali Hassani

PII: S1875-5100(16)30081-6

DOI: 10.1016/j.jngse.2016.02.036

Reference: JNGSE 1286

To appear in: *Journal of Natural Gas Science and Engineering*

Received Date: 31 March 2015

Revised Date: 16 February 2016

Accepted Date: 22 February 2016

Please cite this article as: Safari, A., Dowlatabad, M.M., Hassani, A., Numerical Simulation and X-ray Imaging Validation of Wormhole Propagation during Acid Core-Flood Experiments in a Carbonate Gas Reservoir, *Journal of Natural Gas Science & Engineering* (2016), doi: 10.1016/j.jngse.2016.02.036.

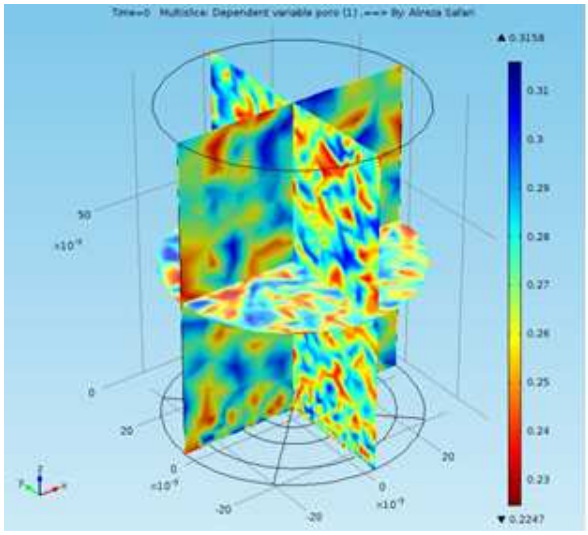

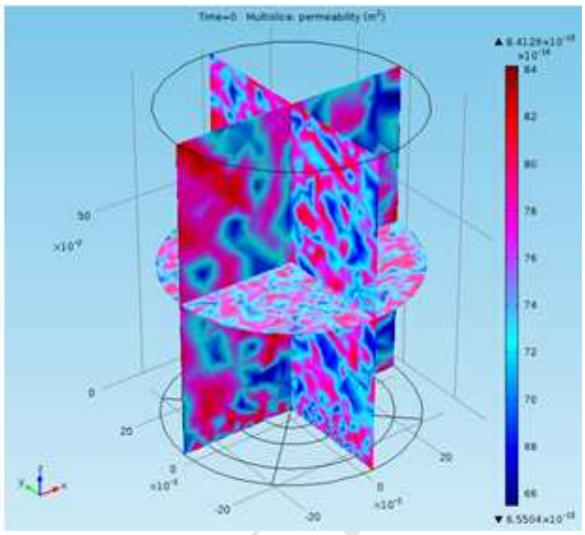

Numerical Simulation and X-ray Imaging Validation of Wormhole Propagation during Acid Core-Flood Experiments in a Carbonate Gas Reservoir

Alireza Safari [a, b], Mojtaba Moradi Dowlatabad [c], Ali Hassani [d]

[a] Mehran Engineering and Well Services Co, Tehran, Iran. E-mail: a.safari@mehranservices.com
[b] Department of Petroleum Engineering, Amirkabir University of Technology, Tehran, Iran. E-mail: a.safari@aut.ac.ir
[c] Institute of Petroleum Engineering, Heriot-Watt University, Edinburgh , UK,E-mail: Mojtaba.moradi@pet.hw.ac.uk
[d] Research Institute of Petroleum Engineering (RIPI), Tehran, Iran. E-mail: hassania@ripi.ir

Abstract

Acidizing is a sophisticated stimulation treatment that significantly improves production rate particularly in the carbonate reservoirs. However, performance evaluation of the treatment requires extensive laboratory experiments. This includes investigation of various parameters such as temperature, pressure, mineralogy of the rock and the effect of chemical diverters in the zones with high contrast permeability (Safari *et al.* (2014). A tuned mathematical model, capable of describing the acidizing in core-scale, can play a vital alternative role due to high expenses of the required experiments. In this paper, we used a simulation model, tuned by experimental data, to be used as an alternative tool for modeling acidization. Since wormhole propagation is strongly geometry dependent, the model was solved in a 3D domain rather than its original dimension, i.e. 2D in Panga (2005) model, to simulate the propagation more accurate.

Mass transfer, continuity, and energy equations were combined to develop a model, which simulates the acid flow in porous media accurately. The model, a cross-link between two different scales: pore-scale and Darcy-scale considers the effect of convection, diffusion, and particularly chemical reactions.

In this study, a complete package including acid core-flood experiment, X-ray imaging and numerical simulation of the wormhole propagation was performed to study acid flow in the porous media. The acid core-flood experiment was performed on a core sample from a gas reservoir in south of Iran. In addition to X-ray imaging technique employed to visualize the result of acid core-flooding, a simulation model was developed in finite element analysis software. The model has the dimensions of the core sample. The required chemical reaction equations were implemented in the simulation model to simulate the wormhole propagation process. A very good agreement was achieved when the simulation results were compared with experimental results and X-ray imaging outputs.

The model, as an invaluable tool could be used to study the different aspects of acidizing treatment such as acid efficiency curve, simulation of parallel flooding, etc. This then helps to determine key parameters and optimized conditions for achieving a successful acidizing treatment.

Keywords: Numerical Model, Acid Core-flood, Carbonate Reservoir, X-ray Imaging, Wormhole

1. Introduction

Generally, all applied sciences are based on conducting experiments and interpreting their results. These experiments are to investigate the impact of various parameters affecting performance of the system. One of the most common methods is to employ an appropriate mathematical model to evaluate effect of individual system variables and their mutual effects. In this study, we used a model that was developed by Panga (2005) to simulate wormhole propagation in the acid-flood experiments in a carbonate gas reservoir.

Many experimental studies such as Fredd *et al.* (1998), Bazin (2001), Safari et al. (2014) investigated the wormholing process and acid efficiency curve. The majority of the studies focused on limestone formation, however, for instance, Fredd and Fogler (1998) showed a significant difference in pore volume to breakthrough curve for the dolomite core used. This kind of difference occurs especially at low temperatures, in which reaction rate in dolomite is much slower than in limestone. The pore scale heterogeneity, which exists because of the different structure of the microbial carbonate, is also reported important by Ziauddin *et al.* (2007). Many other experimental studies investigated various parameters that can affect reaction between acid and rock matrix during any acid-based treatment (Mumallah (1991, Mumallah (1996, Mumallah (1998), Sjoeberg *et al.* (1984), Taylor *et al.* (2006), Taylor *et al.* (2009)).

Since majority of studied core's mineral composition was consisted of calcite (73%) and dolomite (25%) plus very little amount of siderite (>1%), following reactions were the main mechanism of change while acid injection:

$$\text{I) } CaCO_3 + 2HCl \rightarrow CaCl_2 + CO_2 + H_2O \quad (1)$$

$$\text{II) } CaMg(CO_3)_2 + 4HCl \rightarrow CaCl_2 + MgCl_2 + 2CO_2 + 2H_2O \quad (2)$$

$$\text{III) } FeCO_3 + 2HCl \rightarrow FeCl_2 + CO_2 + H_2O \quad (3)$$

Besides the laboratory activities, many other studies were performed to develop models simulating the flow of the acid in porous media.

Steefel et al. (1994) described a numerical model for computing coupled multi-component chemical reactions, multi-species chemical transport, hydrodynamic flow, and heat transfer. Their model employs a new algorithm which solves simultaneously for multi-component reactions and solute transport in one and two dimensions and which uses kinetic formulations for mineral dissolution and precipitation reactions, making the a priori assumption of equilibrium between water and minerals unnecessary.

Liu *et al.* (2013) used a model which couples a two-scale continuum model simulating wormholing in the invaded zone and a reservoir flow model for the compressed zone was used to study the wormhole propagation behavior under reservoir conditions. Their results showed that the normally distributed porosities simulate wormholing better.

Generally, these models can be categorized into four main groups: namely fractal, capillary tube, pore network, and continuum (average) models.

Relating important dimensionless group to experimental observation is a solution that is followed in fractal models (Fredd and Fogler (1998), Fredd (2000), Daccord *et al.* (1987), Frick *et al.* (1994), Pichler *et al.* (1992)).

Capillary tube models are capable of evaluating effect of mass transfer, mutual relation of the wormholes, fluid loss, and reaction on wormhole growth. Interaction and competition between wormholes are key outputs of capillary tube models. Although these models are quite simple, they do not consider the effect of chemical reaction in pore scale as well as transport mechanism. This simplifications may affect the optimum conditions for acidizing (Hung *et al.* (1989), Huang *et al.* (1999), Huang *et al.* (2000), Buijse (2000)).

Pore network model represents porous media in form of many paths that are connected in nodes. Studies performed by Fredd and Fogler (1998) and Hoefner *et al.* (1989) are well-known examples of such modeling. Hagen-Poiseuille relationship describes acid flow in these paths for laminar regime. The acid reaction is considered in form of increase in diameters of these paths. However, scaling up of the result to the field conditions is an issue for these models. Applying such models require large computational power while including heterogeneities effect in pore scale is not usually straightforward.

Due to the deficiencies of first three categories of models, it is generally believed that continuum models are more precise in systematic study of acidizing process. There are three continuum models available: Liu *et al.* (1997), Golfier *et al.* (2002), and Panga (2005). While acid is entering the pores, if the reaction rate is very slow compared to the mass-transfer rate, the concentration gradients are negligible. In this case, the reaction is considered to be in the kinetically controlled regime, and a single concentration variable is sufficient to describe this situation. However, if the reaction is very fast compared to the mass transfer, steep gradients develop inside the pores. This regime of reaction is known as the mass-transfer controlled regime. The Liu et al. (1997)'s model does not take account for mass transfer in reaction and considers chemical reaction at local equilibrium. This model has some limitation to the kinetic regime. The developed model by Golfier et al. (2002) is also available in mass transfer controlled regime. Panga *et al.* (2005) developed a model that overcome drawbacks of two aforementioned models and was infrastructure for many other studies in this area pointed out here. For instance, Izgec *et al.* (2010) explored the effects of heterogeneity on vuggy carbonate acidizing with high resolution computerized tomography imaging, image processing, geostatistical characterization, acid core-flood experiments, and numerical simulations with a continuum approach modeling. De Oliveira *et al.* (2012) developed a methodology to numerically represent the acid treatment in a test plug, as well as to reproduce the different existing dissolution patterns and to obtain the corresponding values of

pore volumes to breakthrough. They used experimental data published by Fredd and Fogler (1998) to justify their simulation results.

Ratnakar *et al.* (2013) used an empirical rheological model to describe the relationship between viscosity of in situ cross-linked acids and temperature, shear rate and pH. They presented a two-scale continuum model to describe reactive dissolution of carbonates with in situ cross-linked acids and to analyze wormhole formation in single and dual core set-ups.

Due to the limitations of the first two models, i.e. Liu et al. (1997) and Golfier et al. (2002) that already discussed, we applied Panga's model for our case. This continuum model, extended to a 3D domain, was solved using a finite element based software and tuned by matching the simulation results with output of X-ray imaging of an acid flooded core from a carbonate gas reservoir in Iran.

2. The Experimental Study Summary and Analysis

Figure 1 illustrates a schematic of the setup used for performing the experiments. Formation water and acid were already put in the accumulators. After putting core sample in Viton sleeves, it was inserted in core-holder. Backpressure, which was supplied by Nitrogen, kept the produced CO_2 during reaction in solution. While injecting, injection rate, temperature, overburden pressure, and back-pressure were kept constant and pressure drop along the core was recorded with digital and analog transducers and converted to appropriate data. Core-holder was placed inside an oven with desired temperature (reservoir temperature (102 ℃)). The Experiment was carried out in reservoir temperature (102 ℃) using HCl 15% wt. (Safari et al. (2014)).

Overburden pressure was kept at least 200 psi greater than inlet pressure in core to prevent fluid from bypassing the core sample during injection. Fluids were kept in corresponding accumulators when a Gilson pump was used to inject fluids at desired rates. Injection was performed at three steps: 1) initial injection of formation water, 2) acid injection, and 3) secondary injection of formation water. The composition of formation water is given in Table 1. During core preparation process, such as cutting, washing, etc. it faced with many changes. Therefore, the reason of injection formation water in first step was to restore the core to its conditions in the reservoir at much as possible.

In the first and third steps, when pressure drop along core samples became steady, core permeability was calculated with known values of pressure drop, injection rate, viscosity, and core geometry. The acid injection step (step 2) was continued up to breakthrough of acid. The breakthrough was identified in two ways: 1) exit of gas from outlet resulted from chemical reaction and 2) change in pH of discharged fluid. The pH of formation water was 5.8, while pH of front of spent acid is about 3-4, therefore this pH drop was considered as breakthrough. During the test, injection rate, back pressure, overburden pressure, inlet and outlet pressure were monitored and recorded as shown in Table 2. (Safari et al. (2014)). The acid breakthrough time

(Here 11 min or 660 seconds, Step 2 in Table 2) was considered as simulation duration. Noting that core-flood experiments are quite time-consuming and expensive; the data produced during these sorts of experiments, might be used as input data in the numerical models that are capable to address behavior of acid flow in porous media. This strategy followed in this paper.

3. Numerical Approach

The Panga's model simulates the linear acid flow in two dimensions. This two-scale continuum model (TSCM) is extended to radial flow in three dimensions in this study while including both the Darcy and pore scale physics in the model. Figure 2 illustrates schematics of the different length scales and geometry used in this study. The mathematical model describes the phenomenon of reactive dissolution as a coupling between processes occurring at the Darcy scale and the pore scale. This model is thoroughly discussed in Appendix A.

The experimental data used in the calculation of acid flow in porous media are divided into two main categories: 1) Rock properties such as porosity and permeability of core samples and the fluids properties such density, viscosity, diffusivity (Table 3). 2) The data that were recorded during core-flood experiment and listed in Table 2.

3.1. The applied software and numerical implementation

A commercial finite element based software that has capability of addressing coupled phenomena applied and a core, having same dimension of the experimental core, with diameter of 2.5 inch and height of 4 inch was modeled in the software. The permeability and porosity of the flooded core sample were measured as 45.72 mD and 0.266 respectively. However, as shown in Figure 3 applying a random function for them provide such distributions of these two parameters. The core's mesh contains 154,229 tetrahedral elements. A fine meshing was applied at the inlet and outlet faces to capture the phenomena occurring near the surfaces. Figure 4 shows the algorithm followed to solve the problem. First, the values of the constant parameters and input of different functions such as the rheological properties of the injected fluid were set. Second, Darcy velocity field and mass transport equations are solved and then porosity field is updated using new concentration of acid obtained. At this step, pore scale equations are related to the Darcy scale ones using new values of porosity and permeability. The cycle shown in Figure 4 starts over from Darcy velocity field calculations. The due time, set for the calculations, is the same as breakthrough time during acid-flood experiment in the laboratory.

4. Simulation Outputs

In following sections, some parameters are discussed that could provide great understanding of acid wormholing in the core.

4.1.1. Pressure Field and Velocity Streamlines

Referring to animation 1 it is clear that as time passes, the pressure iso-surfaces get closer to the core outlet. In other words, the locus of points

with maximum pressure difference gets closer to each other. This is a clear indication of pressure buildup and drawdown due to acid reaction with the matrix of the core. Moreover, as simulation approaches to final time (11 min selected based on experimental data, Table 2); velocity streamlines are more intense in the core center, due to uniform velocity field in core.

4.1.2. Darcy Velocity Field

Another parameter evaluated is the fluid velocity given by Darcy law. This parameter is important due to its role in convection phenomena in mass transfer calculation. Animation 2 shows Z-component of velocity as the Z-direction (V_z) was considered as principal direction of the core in the simulation. It can be seen that velocity iso-surfaces are formed at the core outlet because of low-pressure conditions over there at initial time of the simulation. Later on, the same iso-surface is distributed toward the inlet face resulting in a monotonic distribution of velocity profile at the different sections of the core.

4.1.3. Acid Concentration

Acid concentration evolution in the domain (core sample) as output of mass transfer equation is dynamically shown in animation 3. This parameter plays an important role in porosity equation. As shown in the animation, as simulation approaching to the end, the inlet and center of the core are affected by acid flow more than the other areas.

4.1.4. Reaction Rate

The HCl acid reaction rate with carbonate rock at acid-based treatment operations depends on controllable variables such as injection rate and acid concentration, and variables inherent to the carbonate rock such as permeability, mineral composition, etc. All of them are fed to the continuum model as inputs to be solved using real data from lab. As experimental results were compared with our outputs of X-ray imaging, the reaction rate profile can help to verify the model.

It could be observed from monitoring the reaction rate during simulation that as acid enters the core, reaction rate is high. The reaction rate then decreases as time passes because acid gets weaker. Therefore, the far parts of the core were not affected by the acid flow while the inlet parts were affected as shown in animation 4 and Figure 5.

4.1.5. Peclet Number

In fluid flow, Peclet number as a dimensionless parameter has been extensively utilized to study transport phenomena. Here, it is defined here as ratio of the rate of convection of acid flow to the rate of diffusion of acid, Equation A. 13. The Peclet number was applied to calculate fluid dispersion coefficients.

The variation of this number within the core sample is shown in animation 5. As it could be observed, the pore Peclet number variation is the same in all parts at the beginning. However, by reaching t=500s, when the effect of fluid velocity is increased, pore Peclet number increases in conical path which acid has etched the core matrix.

4.1.6. Reynolds Number

In fluid mechanic, Reynolds number is a dimensionless parameter that relates inertial forces to viscous forces. For a given flow conditions, the Reynolds number quantifies the relative importance of these two forces (Falkovich (2011)). Reynolds number in this model is defined by equation A.11.

Animation 6 demonstrates the acid flow path where Reynolds number increases. In other words, when inertial forces become dominant in a certain path, acid has started to flow in that area.

4.1.7. Sherwood Number

Sherwood number is another dimensionless parameter has been used in mass-transfer operations. Definition of this number, equation A.9, is applied during the acid injection simulation to represent the ratio of convective to diffusive mass transports.

This parameter is more important when it is related to the other two parameters: mass transfer coefficient and Darcy velocity magnitude that are important factors in determining the fluid flow path. The Sherwood initial value is 3, but it increases in conical path of the fluid flow as time passes. This is a clear indication of reaction of acid with core matrix and consequently an increase in mass transfer coefficient. Animation 7 shows the pore Sherwood number variations.

5. Validations

In this section, using available data and tools we tried to evaluate that whether the simulation is close to the experiment or not.

5.1. X-ray Imaging Validation

X-ray computerized tomography (CT) is a non-destructive imaging technique that utilizes X-ray technology and mathematical reconstruction algorithms to view cross-sectional slices of an object. Although CT-scanners are medical diagnostic tools they have been extensively used by oil industry to study the reservoir cores for many years.

In this study, after conducting core-flood experiment, the core sample was X-rayed and image was taken from it. Figures 5 and Figure 6 show this core sample after core-flow experiment and X-ray imaging respectively. As could be seen in this picture, the inlet face of the core to certain depth as well as breakthrough paths were created at the sidewall of the core sample. Video 1 shows 3D projection of core sample by X-ray imaging.

5.2. Porosity Changes

The most indispensable output of this study is porosity variation during the injection time as shown in animation 8. It shows that, as expected, porosity variation happens only in the places where acid flows. An appropriate match between x-ray imaging and model outputs was observed while comparing this animation with video 1.

5.3. Flooding Process: Pressure Changes

To make a true validation, we compared the pressure changes across the core that measured during the experiment with pressure changes predicted by simulation model. As could be seen

in Figure 7, in initial minutes, as arises from relative error, there is a notable difference between simulation and what had been gathered while experiment (Around 11%). But after that period and due to domination of etched path of acid in the core, the result of simulation become closer to the experimental ones and relative error decreased to around -2%.

6. Summary and Conclusion

Pang's model, a continuum model, was used to model acid flow through core samples. Panga's 2D model then was extended to simulate 3D radial behavior of acid wormhole propagation of samples from a carbonated gas reservoir. Different boundary conditions, initial conditions, and core and fluid properties, adopted from the core-flow experiment, were applied to simulate the acid flow behavior using a finite element based software. The flooded core samples were irradiated to x-ray to validate the simulation results and verify the developed model. A great agreement between experiments and simulation was observed. In addition, X-ray imaging provides higher understanding of phenomena happening during acid wormhole propagation.

The developed model could be used as an invaluable alternative than conventional expensive and cumbersome laboratory experiments for studying the different aspects of acidizing treatment such as wormhole efficiency curve, parallel flooding simulation, etc. This could be used to determine key parameters and optimized conditions for achieving a successful acidizing treatment .

Acknowledgement

This work was part of a M.Sc. thesis entitled "Study, Evaluation, and modeling of wormhole propagation during matrix acidizing carbonate reservoirs". We would like to thank Amirkabir University of Technology and Research Institute of Petroleum Industry (RIPI) for their support and permission to publish the study.

References

Bazin, B. (2001). "From matrix acidizing to acid fracturing: A laboratory evaluation of acid/rock interactions." SPE Production & Facilities **16**(01): 22-29.

Buijse, M. A. (2000). "Understanding wormholing mechanisms can improve acid treatments in carbonate formations." SPE Production & Facilities **15**(03): 168-175.

Daccord, G. and R. Lenormand (1987). "Fractal patterns from chemical dissolution." Nature **325**(6099): 41-43.

De Oliveira, T. J. L., et al. (2012). Numerical Simulation of the Acidizing Process and PVBT Extraction Methodology Including Porosity/Permeability and Mineralogy Heterogeneity. SPE International Symposium and Exhibition on Formation Damage Control, Society of Petroleum Engineers.

Falkovich, G. (2011). Fluid mechanics: A short course for physicists, Cambridge University Press.

Fredd, C. (2000). Dynamic model of wormhole formation demonstrates conditions for effective skin reduction during carbonate matrix acidizing. SPE Permian Basin Oil and Gas Recovery Conference, Society of Petroleum Engineers.

Fredd, C. N. and H. S. Fogler (1998). "Influence of transport and reaction on wormhole formation in porous media." AIChE Journal **44**(9): 1933-1945.

Frick, T. P., et al. (1994). "Modeling of Fractal Patterns in Matrix Acidizing and Their Impact on Well Performance." SPE Production & Facilities.

Golfier, F., et al. (2002). "On the ability of a Darcy-scale model to capture wormhole formation during the dissolution of a porous medium." Journal of fluid mechanics **457**: 213-254.

Hoefner, M. and H. Fogler (1989). "Fluid-velocity and reaction-rate effects during carbonate acidizing: application of network model." SPE production engineering **4**(01): 56-62.

Huang, T., et al. (2000). "Reaction rate and fluid loss: The keys to wormhole initiation and propagation in carbonate acidizing." SPE Journal **5**(03): 287-292.

Huang, T., et al. (1999). Prediction of wormhole population density in carbonate matrix acidizing. European formation damage conference.

Hung, K., et al. (1989). "A mechanistic model of wormhole growth in carbonate matrix acidizing and acid fracturing." J. Petrol. Technol **41**(1): 59-66.

Izgec, O., et al. (2010). "Numerical and experimental investigation of acid wormholing during acidization of vuggy carbonate rocks." Journal of Petroleum Science and Engineering **74**(1): 51-66.

Liu, M., et al. (2013). "Wormhole propagation behavior under reservoir condition in carbonate acidizing." Transport in porous media **96**(1): 203-220.

Liu, X., et al. (1997). "A geochemical reaction-transport simulator for matrix acidizing analysis and design." Journal of Petroleum Science and Engineering **17**(1): 181-196.

Mumallah, N. (1991). Factors influencing the reaction rate of hydrochloric acid and carbonate rock. SPE International Symposium on Oilfield Chemistry, Society of Petroleum Engineers.

Mumallah, N. A. (1996). "Hydrochloric acid diffusion coefficients at acid-fracturing conditions." Journal of Petroleum Science and Engineering **15**(2): 361-374.

Mumallah, N. A. (1998). "Reaction rates of hydrochloric acid with chalks." Journal of Petroleum Science and Engineering **21**(3): 165-177.

Panga, M. K., et al. (2005). "Two-scale continuum model for simulation of wormholes in carbonate acidization." AIChE Journal **51**(12): 3231-3248.

Panga, M. K. R. (2005). Multiscale Transport and Reaction: Two Case Studies. Chemical Engineering, University of Houston. **PhD:** 218.

Pichler, T., et al. (1992). Stochastic Modeling of Wormhole Growth in Carbonate Acidizing With Biased Randomness. European Petroleum Conference. Cannes, France, SPE.

Ratnakar, R. R., et al. (2013). "Modeling, analysis and simulation of wormhole formation in carbonate rocks with in situ cross-linked acids." Chemical Engineering Science **90**: 179-199.

Safari, A., et al. (2014). "Determining optimum acid injection rate for a carbonate gas reservoir and scaling the result up to the field conditions: A case study." Journal of Natural Gas Science and Engineering **20**: 2-7.

Sjoeberg, E. L. and D. T. Rickard (1984). "Calcite dissolution kinetics: surface speciation and the origin of the variable pH dependence." Chemical Geology **42**(1): 119-136.

Steefel, C. I. and A. C. Lasaga (1994). "A coupled model for transport of multiple chemical-species and kinetic precipitation dissolution reactions with application to reactive flow in single-phase hydrothermal systems." American Journal of science(294): 529-592.

Taylor, K. and H. Nasr-El-Din (2009). "Measurement of acid reaction rates with the rotating disk apparatus." Journal of Canadian Petroleum Technology **48**(6): 66-70.

Taylor, K. C., et al. (2006). "Anomalous acid reaction rates in carbonate reservoir rocks." SPE Journal **11**(04): 488-496.

Ziauddin, M. E. and E. Bize (2007). The Effect of Pore Scale Heterogeneities on Carbonate Stimulation Treatments. SPE Middle East Oil and Gas Show and Conference, Society of Petroleum Engineers.

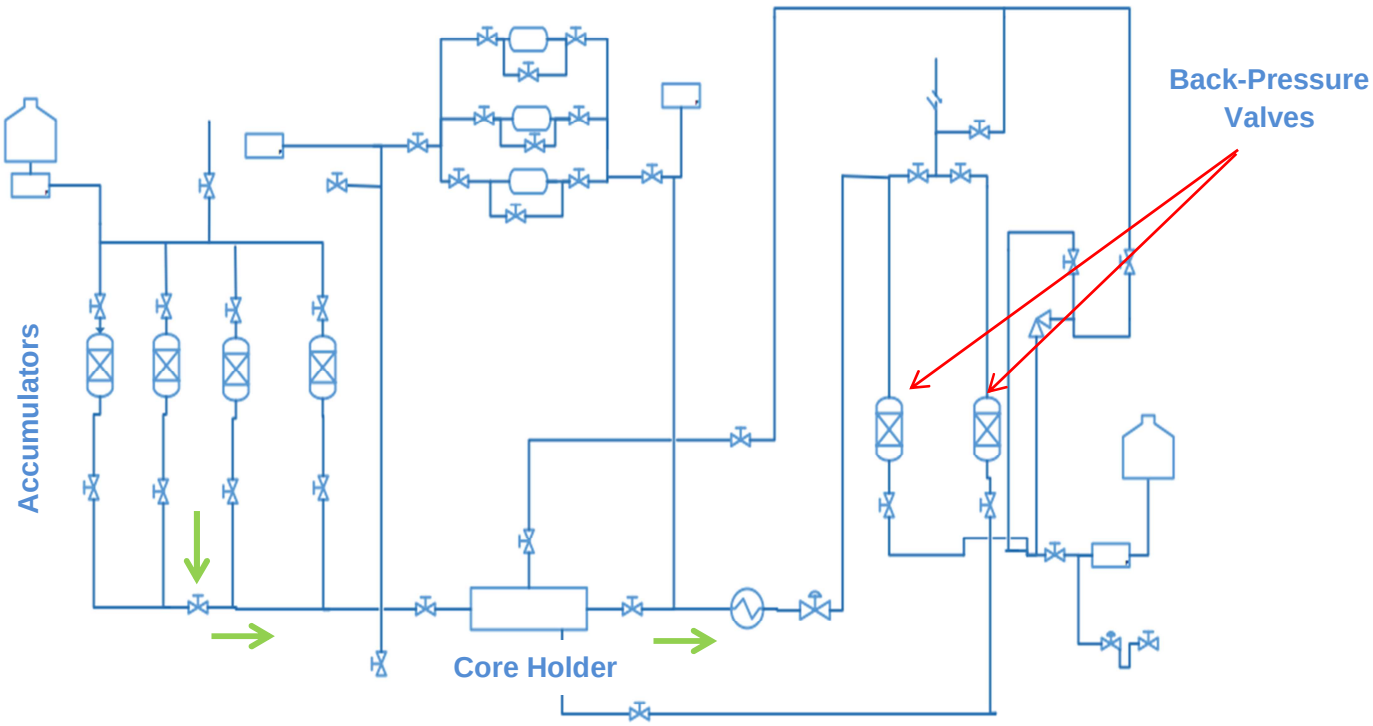

Fig.1. Schematic of experimental setup used during experiments. The green arrows show the direction of flow.

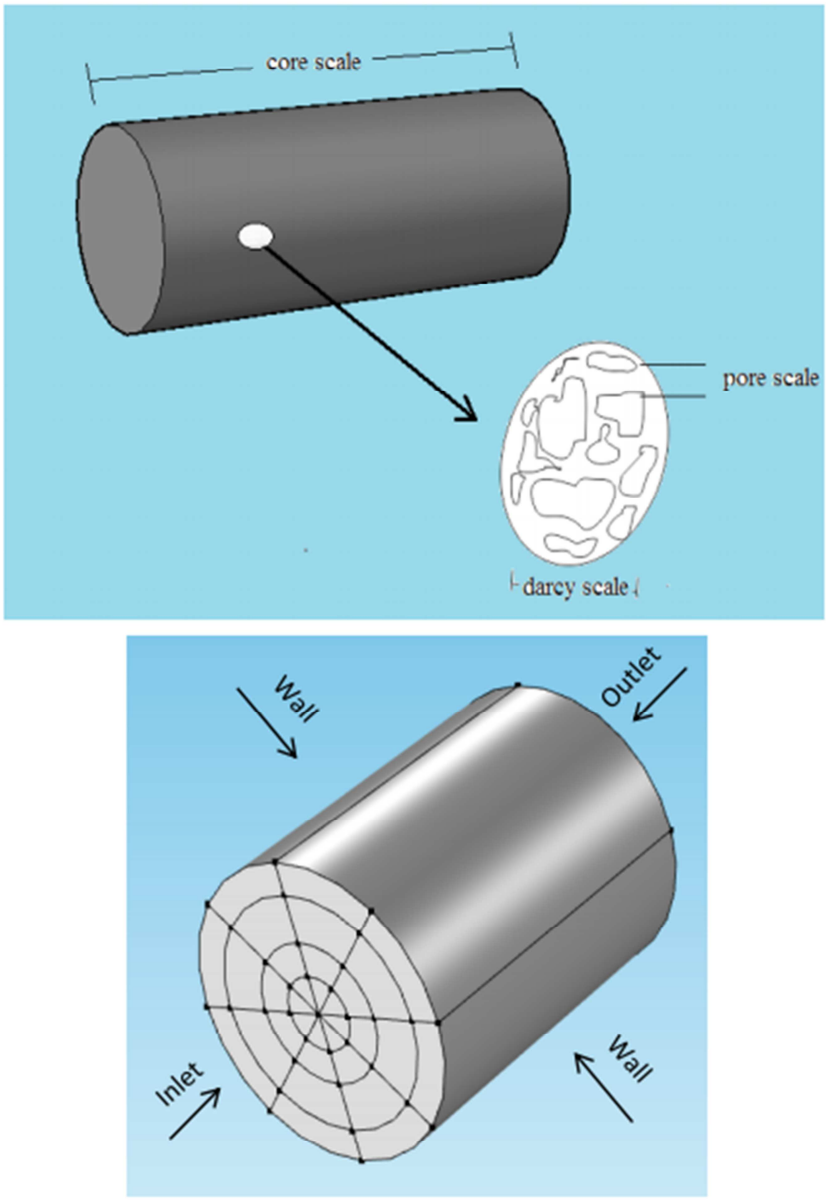

Fig.2. Schematic of different scales in porous media (up) and 3-D domain with boundary conditions viewpoint (down)

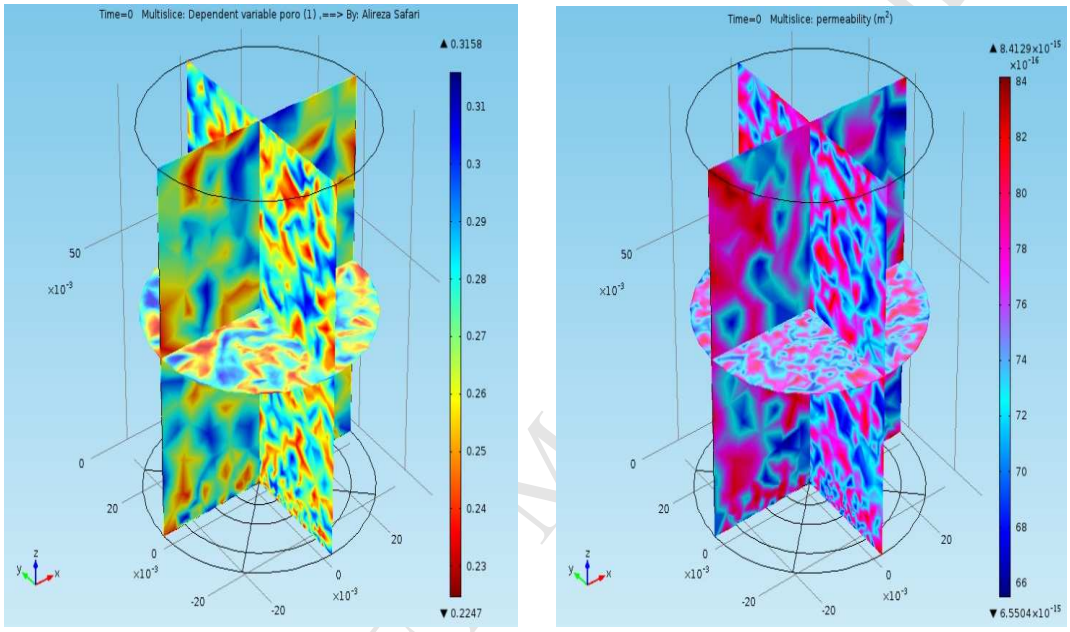

Fig.3. Initial porosity (Left) and permeability (Right) distribution in the core sample model.

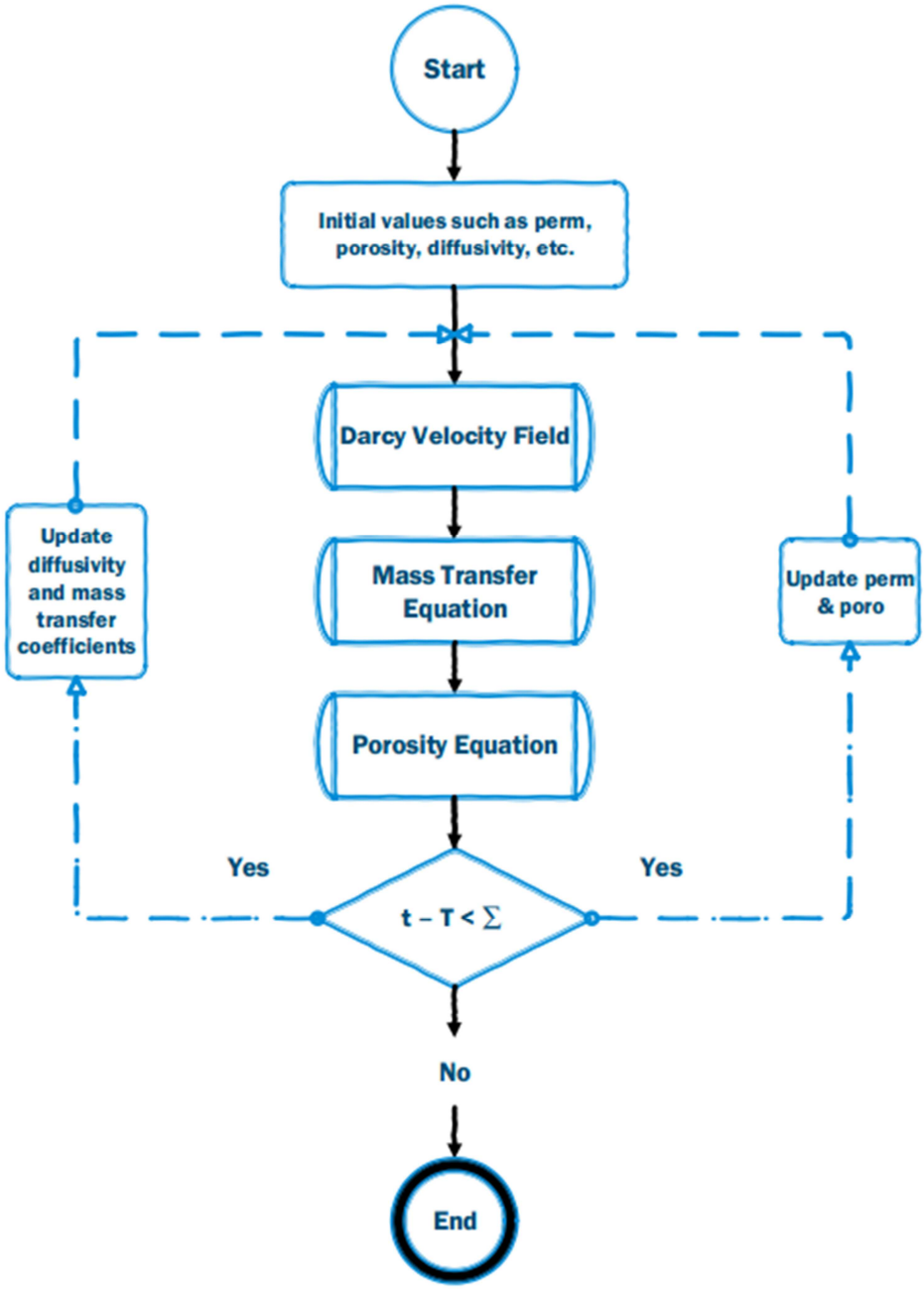

Fig.4. Flowchart applied to solve model's equation system. ∑ in above flowchart is constant and equals to 1e-06

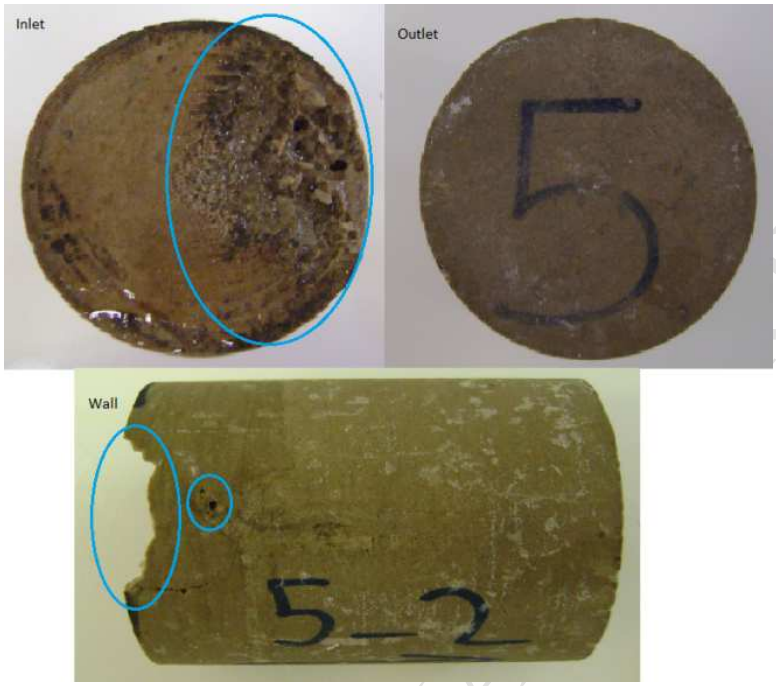

Fig.5. Acid flooded core sample used in this study. Inlet face, outlet face and lateral areas of the core are shown after flooding by acid

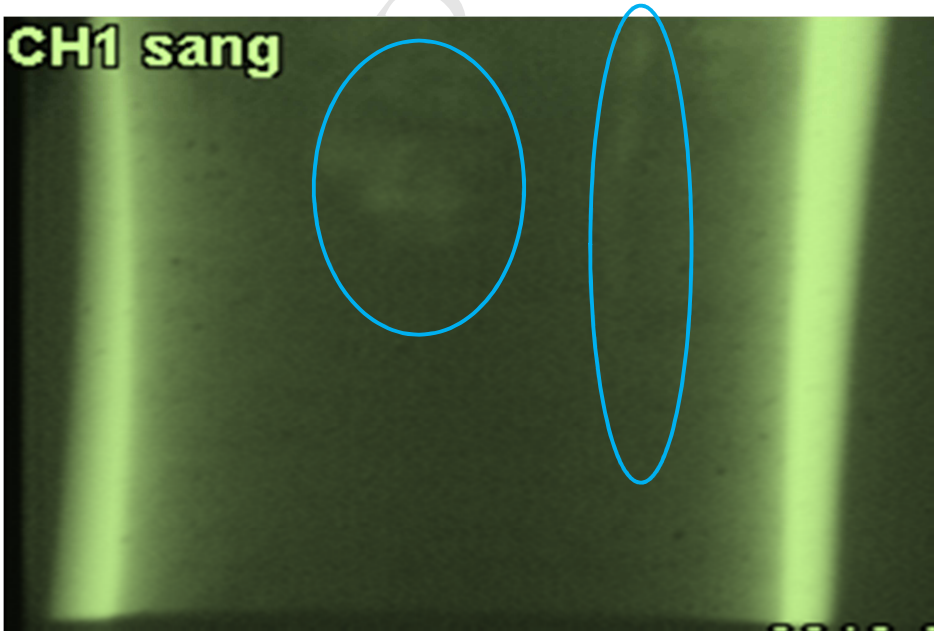

Fig.6. The flooded core sample after exposing to X-ray, blue ovals show the places that are etched by acid

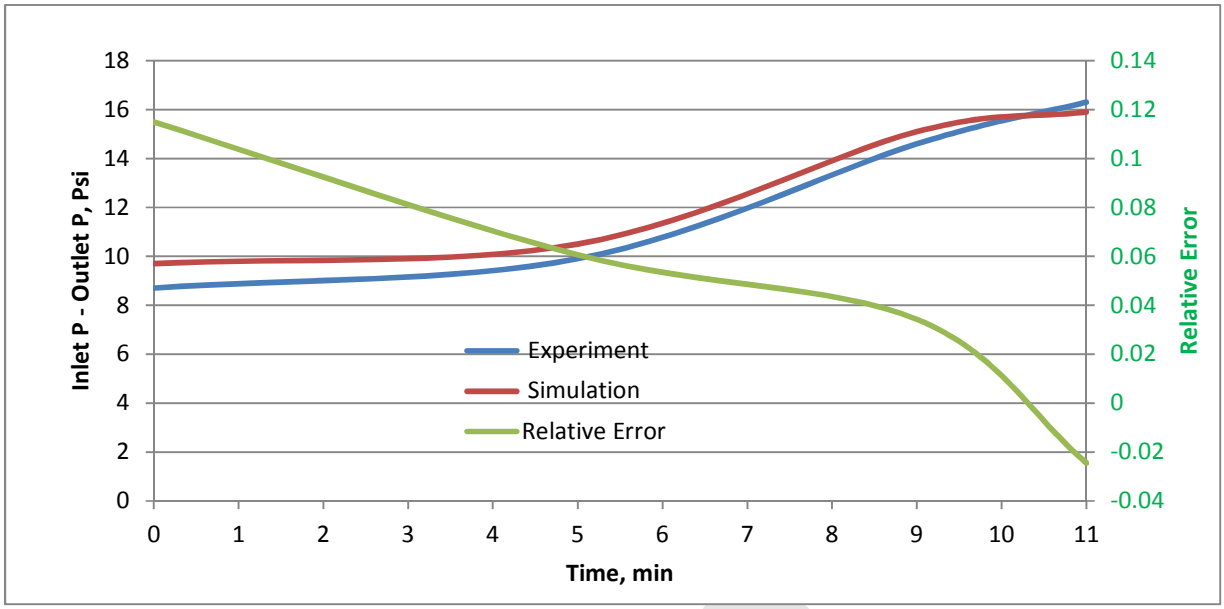

Fig.7. Comparison of pressure changes across the core: Simulation vs. Experiment

Table 1. Standard 10-ion water analysis for dead formation water sample

Specific gravity at 60/60 ºF : 1.193 pH at 75 °F : 5.8 Resistivity @ 75 ºF (ohm-meter) : 0.042 Total Dissolved Solids (mg/L) : 294982		
Cations	Mg/l	Meq/l
Sodium	72050	3132.6
Calcium	29594	1479.70
Magnesium	2902	238.9
Iron	0.6	0.02
Barium	ND	ND
Potassium	8681	222.6
Strontium	1522	34.8
Manganese	0	0.02
Fe3+	0.6	0.02
Anions	Mg/l	Meq/l
Chloride	179525	5064.2
Bicarbonate	134	2.2
Sulphate	354	7.4
Carbonate	0	0
Hydroxide	0	0

Table 2. Time and pressure boundary conditions data

No	Stage	Time (min)	Injection rate (cc/min)	Back Pressure (bar)	Overburden Pressure ** (bar)	Inlet Pressure (bar)	Outlet Pressure (bar)
1	Initial Formation Water Injection	0	1	~50	60	51.8	49.9
		10	1	~50	60	51.9	50.2
		20	1	~50	60	52	50.2
		30	1	~50	60	52.1	50.3
		40	1	~50	60	52.1	50.4
		50	1	~50	60	51.9	50.2
		60	1	~50	60	52.1	50.5
2	Acid Injection	0	5	~50	70	59.5	50.8
		5	5	~50	70	60.9	51
		9	5	~50	72	65.5	50.9
		11	5	~50	75	67.1	50.8
3	Final Formation Water Injection	0	1	~50	70	62.3	50.4
		10	1	~50	65	55.6	50.7
		15	1	~50	65	54	50.8
		20	1	~50	65	53.7	50.5
		25	1	~50	65	59.8	50.7
		35	1	~50	65	52.5	50.2
		40	1	~50	65	55.3	50.8
		45	1	~50	65	59.9	50.9

**) Changing overburden pressure is direct consequence of reaction of acid with rock. To keep the injection rate in desired value, we let the overburden pressure to vary.

**) As could be seen, the pressure drop from 16.3 bar (67.1-50.8) has reached to 11.9 bar (62.3-50.4) right after breakthrough. This 4.4 bar change in pressure drop is obvious indication of wormholing.

Table 3. Model parameters and corresponding values

K_0	φ_0	μ	k_s	D_m	ρ_s	ρ_f	C_{ini}	a_0	r_0
7.48e-15	0.27	1.23e-3	2e-4	4e-6	2726	1069.7	4745.15	124.64	4.48 e-7
m^2	-	Pa.s	m/s	m^2/s	kg/m^3	kg/m^3	mole/m^3	1/m	m

Appendix A

The Panga (2005)'s mathematical model describes the phenomenon of reactive dissolution as a coupling between processes occurring at the Darcy scale and the pore scale. These processes based on his work are shortly addressed in upcoming sections.

The Darcy scale model equations are given by:

1. Darcy Scale

Following equations show Darcy scale model:

$$\mathbf{U} = \frac{-\mathbf{K}}{\mu}\nabla\mathbf{P} \quad \text{A.1}$$

$$\frac{\partial\varphi}{\partial t} + \nabla\mathbf{U} = \mathbf{0} \quad \text{A.2}$$

$$\varphi\ \frac{\partial \mathbf{C_f}}{\partial t} + \mathbf{U}.\nabla\mathbf{C_f} = \nabla.(\varphi\mathbf{D_e}\nabla\mathbf{C_f}) - \mathbf{k_c a_v}(\mathbf{C_f} - \mathbf{C_s}) \quad \text{A.3}$$

$$\mathbf{k_c}(\mathbf{C_f} - \mathbf{C_s}) = \mathbf{R}(\mathbf{C_s}) \quad \text{A.4}$$

$$\frac{\partial\varphi}{\partial t} = \frac{\mathbf{R}(\mathbf{C_s})\alpha.\mathbf{a_v}}{\rho_s} \quad \text{A.5}$$

Transport of the acid species in Darcy scale is described in Equation A.3. Accumulation, convection and dispersion of the acid are the first three terms in the equation, respectively. Transfer of acid species from the fluid phase to the fluid-solid interface is considered in the fourth term and its role is discussed later in this section. Darcy's law (Eq. A. 1), relating velocity to the permeability field K and the gradient of pressure, is used to obtain velocity field, U, in the convection term. The effect of change in local volume during dissolution on the flow field is considered in the first term in the continuity equation, Eq. A. 2 There is this assumption that, the dissolution process does not lead to a significant change in the density of the fluid phase. The transfer term in the species balance Eq. A. 3 describes the depletion of the reactant at the Darcy scale due to reaction. The description of transport and reaction mechanisms affects accurate estimation of this term inside the pores. Reaction at the solid-fluid interface gives rise to concentration gradients in the fluid phase inside the pores. The relative rate of mass transfer from the fluid phase to the fluid-solid interface and reaction at the interface will control magnitude of these gradients. To account for the gradients developed due to mass transfer control requires the solution of a differential equation describing diffusion and reaction mechanisms inside each of the pores. Since this is impractical, Panga (2005) used two concentration variables C_s and C_f, for the concentration of the acid at the fluid-solid interface and in the fluid phase respectively, and capture the information contained in the local concentration gradients as a difference between the two variables using the concept of a local mass transfer coefficient (Eq. A. 4). The change in local porosity due to dissolution phenomena is described via an additional equation that is derived from balance between amount of dissolved rock and consumed acid. This equation is given in Eq. A. 5.

2. Pore Scale

The pore scale equations are divided to three categories that are shown in following sections:

2.1. Structure-Property Relation

Dissolution changes the structure of the porous medium continuously, thus, making it difficult to correlate the changes in local permeability to porosity during acidization. The results obtained from averaged models, which use

these correlations, are subject to quantitative errors arising from the use of a bad correlation between the structure and property of the medium, although the qualitative trends predicted may be correct. Since a definitive way of relating the change in the properties of the medium to the change in structure during dissolution does not exist, we use semi-empirical relations that relate the properties to local porosity. The relative increase in permeability, pore radius and interfacial area with respect to their initial values are related to porosity in the following manner (Panga (2005)):

$$\frac{K}{K_0} = \frac{\varphi}{\varphi_0}\left(\frac{\varphi(1-\varphi_0)}{\varphi_0(1-\varphi)}\right)^{2\beta} \quad \text{A.6}$$

$$\frac{r_p}{r_0} = \sqrt{\frac{K\varphi_0}{K_0\varphi}} = \left(\frac{\varphi(1-\varphi_0)}{\varphi_0(1-\varphi)}\right)^{\beta} \quad \text{A.7}$$

$$\frac{a_v}{a_0} = \frac{\varphi r_0}{\varphi_0 r_p} = \frac{\varphi}{\varphi_0}\left(\frac{\varphi(1-\varphi_0)}{\varphi_0(1-\varphi)}\right)^{-\beta} \quad \text{A.8}$$

2.2. Mass Transfer Coefficient

Transport of the acid species from the fluid phase to the fluid-solid interface inside the pores is quantified by the mass-transfer coefficient (kc). It plays an important role in characterizing dissolution phenomena because the mass-transfer coefficient determines the regime of reaction for a given acid. The mass-transfer coefficient depends on the local pore structure, reaction rate and local velocity of the fluid (Panga (2005)).

$$\mathbf{Sh} = \frac{2k_c r_p}{D_m} = \mathbf{Sh}_\infty + \frac{0.7}{\sqrt{m}}\mathbf{Re}_p^{\,0.5}\mathbf{Sc}^{1/3} \quad \text{A.9}$$

$$\rightarrow \mathbf{k_c} = \frac{\mathbf{Sh} * D_m}{2r_p} \quad \text{A.10}$$

In addition, Schmidt number and Reynolds number are defined as follows:

$$\mathbf{Re_p} = \frac{2U\, r_p}{\nu} \quad \text{A.11}$$

$$\mathbf{Sc} = \frac{\mu}{\rho D_m} \quad \text{A.12}$$

2.3. Fluid Dispersion Coefficients

In this section, longitudinal and transversal diffusivity variables desired for solving equation A.3 are defined using Peclet number. In each iteration during simulation, since $|\mathbf{U}|$ and φ are changing, Pe_p and diffusivity variables will be updated (Panga (2005)).

$$\mathbf{Pe_p} = \frac{|U| d_h}{\varphi D_m} \quad \text{A.13}$$

$$\mathbf{D_X} = \alpha_{os} + \lambda_X \mathbf{Pe_p} \quad \text{A.14}$$

$$\mathbf{D_T} = \alpha_{os} + \lambda_T \mathbf{Pe_p} \quad \text{A.15}$$

3. Boundary and Initial Conditions

Table 4 shows boundary conditions applied to solve the equations. Initial concentration of acid in domain was set to zero. Random distributions function of porosity, permeability, and acid concentration in the inlet face were considered to include effect of heterogeneity (Panga (2005)).

Table 4. The applied boundary conditions for calculations

Boundary Conditions	
Darcy law	Species Transport
$-\frac{k}{\mu}.\nabla P = U_0$ @ Inlet $P = P_{out}$ @ Outlet $-k.\nabla P = 0$ @ Walls	$-n.C_i = C_{ini}$ @ Inlet $C = 0$ @ Outlet & Walls *

*) This means that due to sleeve around the core during injection, there was not any acid there.

Nomenclature

a_0: Initial interfacial area per unit volume [1/m]

a_v: Interfacial area per unit volume [1/m]

C_{ini}: Initial acid concentration [mole/m^3]

C_f: Acid concentration [mole/m^3]

C_s: Acid concentration in liquid-solid interface [mole/m^3]

d_h: Pore hydraulic diameter[m]

D_m: Molecular diffusivity of acid [m^2/s]

D_e: Dispersivity tensor [m^2/s]

D_X: Longitudinal dispersivity [m^2/s]

D_T: Transversal dispersivity [m^2/s]

k_c: Mass transfer coefficient [m/s]

k_s: Surface reaction constant [m/s]

K: Permeability tensor [m^2]

K_0: Initial permeability of domain [m^2]

m: ratio of pore length to pore radius[-]

P: Pressure [Pa]

P_{out}: Outlet pressure at core face [Pa]

Pe_p: Pore Peclet number [-]

r_p: Pore radius[m]

r_0: Initial pore radius[m]

Re_p: Pore Reynolds number [-]

Sc: Schmidt number [-]

Sh: Sherwood number [-]

Sh_∞: Asymptotic Sherwood number [-]

U: Darcy velocity vector [m/s]

|U|: Magnitude of Darcy velocity vector [m/s]

α: Acid dissolving power [-]

α_{os}: Empirical constant [m^2/s]

β: Empirical constant

λ_X: Empirical constant [m^2/s]

λ_T: Empirical constant [m^2/s]

φ: Porosity [-]

φ_0: Initial porosity [-]

μ: Acid viscosity [Pa.s]

v: Acid kinematic viscosity [m^2/s]

ρ_s: Rock density [kg/m^3]

ρ_f: Acid density [kg/m^3]

Highlights:

- We tried to simulate acid flow through a core sample from a carbonate gas reservoir
- Data from core-flow experiment was used to justify simulation results
- A developed 2-D continuum model was solved in 3-D domain
- The flooded core, was x-rayed to understand prediction capability of the model
- A very good agreement between experiments and simulation was observed